International Investment Agreements and FDI inflows in Africa

Preliminary Analysis on Environmental and Intrinsic Factors on FBG-Based Vibration Sensors

To cite this article: Gaetano Quattrocchi *et al* 2021 *J. Phys.: Conf. Ser.* **1977** 012011

Preliminary Analysis on Environmental and Intrinsic Factors on FBG-Based Vibration Sensors

Gaetano Quattrocchi, Matteo Davide Lorenzo Dalla Vedova, Pier Carlo Berri, Paolo Maggiore

Department of Mechanical and Aerospace Engineering (DIMEAS) - Politecnico di Torino, Corso Duca degli Abruzzi 24, 10129, Turin, Italy

E-mail: `matteo.dallavedova@polito.it`

Abstract. In recent years, optical-based sensors have sparked interest for the many advantages over traditional, electrical-based sensors, such as EMI insensitivity, ease of multiplexing on a single line, resilience to hostile environment and very compact size and global weight saving due to signal cables reduction. Considering said properties, optical sensors offer a compelling alternative to traditional sensing elements. One type of optical sensor is the Fiber Braggs Gratings sensors (FBG), which is a type of sensor that reflects a very narrow band of wavelengths, called Bragg wavelength, while being transparent for others; this behavior is achieved by local variations of the core refractive index. The Bragg wavelength can be easily correlated with physical changes in the sensor itself, due to either physical strain or temperature variation. It should be noted that the achievable measurement accuracy is thus comparable to the Bragg wavelength. However, for any practical application, FBGs need to be bonded to a support or surface; in this case, there is a lack of understanding of the effects of temperature and humidity variations on the combined sensor-glue system. In this work, a setup, intended to characterize the sensitivity of the fiber-glue combination to humidity and temperature will be presented.

1. Introduction

Prognostics algorithms operate on a series of values, so called precursors, to identify any potential anomaly before it hinders the ability to operate of a component or system; whenever that threshold is crossed, Fault Detection and Isolation (FDI) and thus diagnostics are the domain of interest.

Often prognostics algorithms leverage machine learning, as in [1, 2, 3], thus requiring a large amount of data to correctly predict the current health status of the system and possibly to estimate the Remaining Useful Life (RUL) of the component or system. On the other hand, model-based approaches are also possible as presented in [4, 5, 6] or even a combination of both as in [7, 8]. Furthermore, such sensors need to have low noise and high robustness to have a realistic prediction of the system status [9]. In fact, as reported in [10], the accuracy of a prognostics algorithm can be directly derived from the accuracy of the data provided and thus to the sensors accuracy.

Especially for mechanical or even aerospace systems, the installation of sensors could possibly prove difficult or counterproductive given the increase in mass, bulk and complexity associated with the integration of several sensors to log various quantities of interest (accelerations, forces, temperatures, etc.). In this context, optical-based sensors can prove very useful given their characteristics: lightness, small sizes, EMI insensitivity, harsh environments tolerance [11] and multiplexing capability of tens or hundreds of sensors on a single optical line [12]. This last capability, i.e. the ability to have a large number of sensing elements on a single optical line is a powerful tool that can be leveraged to obtain a distributed sensing network with high spatial resolution.

One interesting kind of optical sensor is the Fiber Bragg Gratings (FBG). The principle of operation of FBGs is relatively simple: a diffraction grating is inscribed in the fiber core, which then reflects a very narrow band of wavelength, called the Bragg wavelength. Variation in Bragg wavelength can be correlated to physical strain of the fiber, due either to stress or temperature variation, as reported in [13]. Practical applications have been reported for example in [14, 15], including vibration sensors as in [16], pressure sensors as in [17] or even mulit-axial forces as in [18].

However, it is difficult to separate the contribution given by temperature and physical stress. In the simple case where temperature fluctuations are very small or negligible, the mechanical deformation can be assumed to be zero or can be compensated via sensor calibration [19]. On the other hand, in cases where temperature (or humidity) fluctuations are significant, a reliable estimation of the environmental parameters is needed in order to operate on the raw sensed data [20]. Again, the correct correlation between Bragg wavelength and environmental factors is essential to achieve a good and reliable measurement of the quantities of interest.

In this context, the paper aims at presenting a new test bench whose scope will be to characterize the behavior of fiber-glue system at various temperatures and humidity.

2. FBGs principles of operation

As previously stated, Fiber Bragg Gratings optical fiber sensors allow the measuring of a large number of different physical quantities with minimal encumbrance and very light weight [21]. In essence, the FBG itself is composed by a series of periodical variation of the refractive index of the core of the fiber, thus it is an embedded element; physical length is in the millimeter range. There are various technique used to generate the periodical pattern, but the most prevalent is the UV interference method. In this technique, the fiber is photosensitive, generally made of germanium-doped glass. By opportune manipulation of the interference pattern of two UV light sources, a grating can be thus inscribed in a segment of fiber.

The grating can be thought as of a wavelength-specific dielectric mirror [22], i. e. most wavelengths passing through the grating are transmitted, while a small windows is reflected back. The physical phenomenon behind FBGs is Fresnel reflection.

The main equation describing the Bragg wavelength is:

$$\lambda_B = 2n_{eff} \cdot \Lambda \tag{1}$$

where λ_B is the Bragg wavelength, n_{eff} is the refractive index and Λ is the grating pitch.

As previously described, FBGs can be used as strain and/or temperature sensors. The variation of temperature ΔT or physical strain $\Delta\varepsilon$ affect both the fiber refractive index and the physical pitch of the grating. Thus, the effects on the Bragg wavelength can be described as:

$$\Delta\lambda_B = \lambda_B(1 + p_E)\Delta\varepsilon + \lambda_B(\alpha_\Lambda + \alpha_n)\Delta T \tag{2}$$

where the following terms appear: λ_B, Bragg wavelength; p_E, fiber strain-optic coefficient; $\Delta\varepsilon$, fiber strain variation; α_Λ, fiber thermal expansion coefficient; α_n, fiber thermo-optic coefficient; ΔT, temperature variation.

Equation 2 can be rewritten as:

$$\Delta\lambda_B = K_\varepsilon\Delta\varepsilon + K_T\Delta T \tag{3}$$

where the coefficients K_ε and K_T are referred to as coefficient of strain and coefficient of temperature, respectively.

It follows that:

$$K_\varepsilon = \lambda_B(1 + p_E) \tag{4}$$

$$K_T = \lambda_B(\alpha_\Lambda + \alpha_n) \tag{5}$$

It has to be noted that said coefficients are calculated for a free fiber not glued or constrained to a support. Regarding K_ε, it describes the variation of refractive index of the fiber undergoing a normal (i.e. axial) stress. Since the value is derived from the optical strain coefficient, it depends on the material used for the fiber making; conventional value of the optical strain coefficient is assumed as $p_e = -0.212$.

The coefficient K_T is instead composed of two parameters: the first is the thermo-optic coefficient, which is a measure of the variation of the fiber refractive index as function of the temperature variation; it is thus dependent on the fiber material and thus it is supposed to be constant for different applications. Generally, for glass fibers, the value is $\alpha_n = 5.77 \cdot 10^{-6}\ {}^oC^{-1}$.

The other parameter is the thermal dilation coefficient, which relates temperature variations to the physical disposition of the grating. In fact, an increase in temperature leads to an expansion of the glass itself and thus to an increase in spacing of the grating, thus increasing the Bragg frequency. For a glass fiber not glued or constrained to a support, the value assumed is that of glass, i.e. $\alpha_\Lambda = 0.55 \cdot 10^{-6}\ {}^oC^{-1}$.

Regarding the humidity variation on the Bragg wavelength, it is assumed that the naked fiber is not sensitive to humidity variation. However, in presence of a polymer cover, which is almost always the case, there is an appreciable effect on the variation of Bragg wavelength as function of the relative humidity variation. The effect can be explained as an increase in fiber strain due to dilation of the polymeric covering that has absorbed moisture from the air. Since the relation between relative humidity variation and Bragg wavelength is almost ascribable to the properties of the fiber cover, it is generally calibrated on a per-case basis, given the enormous variability in cover material and thickness. The same principle is used to create gas-sensing FBG-based elements: an appropriate absorbing coating material is used to induce a strain on the FBG itself as function of the gas concentration, and thus to indirectly measure the amount of gas in the atmosphere.

3. Experimental setup description

In this section, the experimental setup that will be used for long-term data logging of environmental conditions and Bragg wavelength will be described. The scope of the work will be to analyze and characterize any possible time-dependent, non-linear phenomena arising from the FBGs bonding to the support using glue.

3.1. Measuring stations

In Fig. 1, the conceptual schematics of the testing setup is reported. Three different data logging stations are present, respectively called by the authors "Fridge", "Table" and "Radiator"; each one of the stations has the scope to analyze the behavior of the FBGs-support combinations in different operating conditions, at various values of temperature and relative humidity. In particular, no thermal conditioning is applied on the "Table" station (i.e. is kept at room temperature), while the "Fridge" station is held at sub-ambient temperature and "Radiator" is, on the other hand, kept above room temperature. "Radiator" and "Fridge" measuring stations are depicted in Fig. 2a and Fig. 2b, respectively. In particular, "Fridge" setup is placed in a refrigerated environment characterized by shallow temperature and humidity excursions; it has a thermal range of about 2 ^oC (nominally from $-1\ {}^oC$ to $+1\ {}^oC$). The second setup, "Table", is

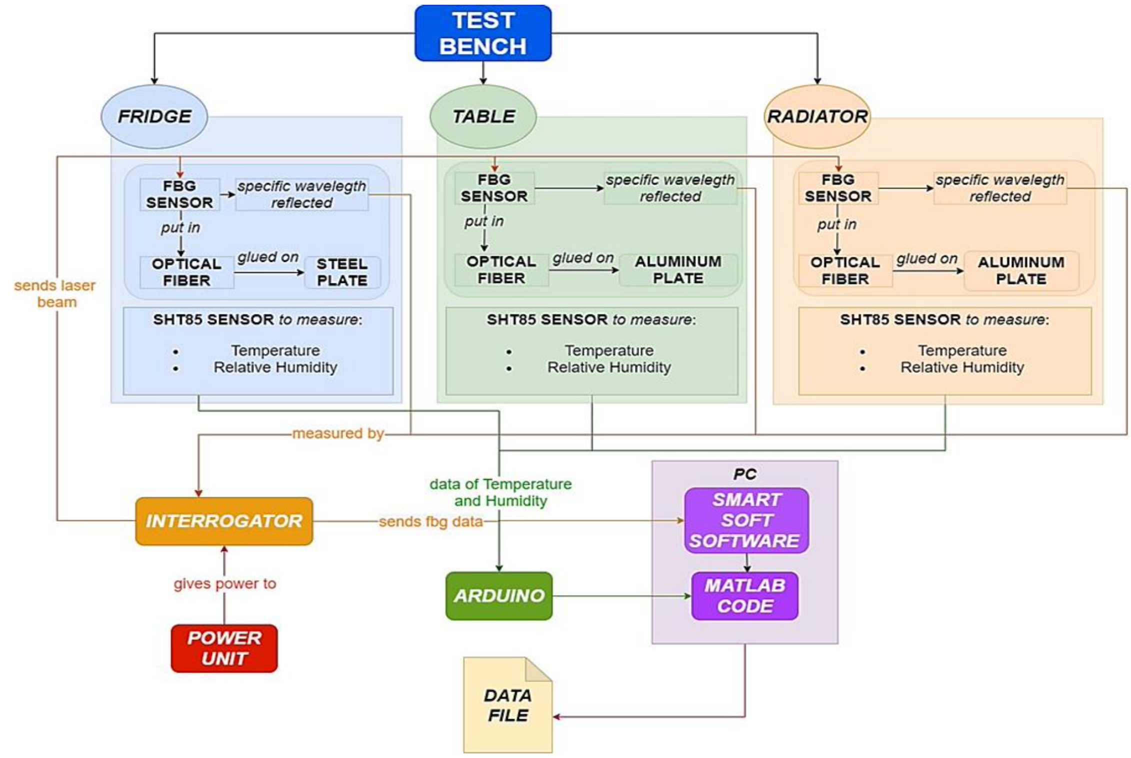

Figure 1: Conceptual schematics of the testing setup

positioned in the laboratory and, therefore, measures the environmental test conditions (linked to the weather changes and anthropogenic effects). The third station, "Radiator", was placed near a convector (used for heating one of the laboratory rooms) to be subject to periodic and significant variations in temperature and ambient humidity.

3.2. Setup components

The main components of the test bench are: three optical fibers with FBG sensors, mechanical support frames, the FBG optical interrogator, electrical power unit, SHT85 temperature and humidity sensors, ARDUINO UNO microcontroller, PC for data saving.

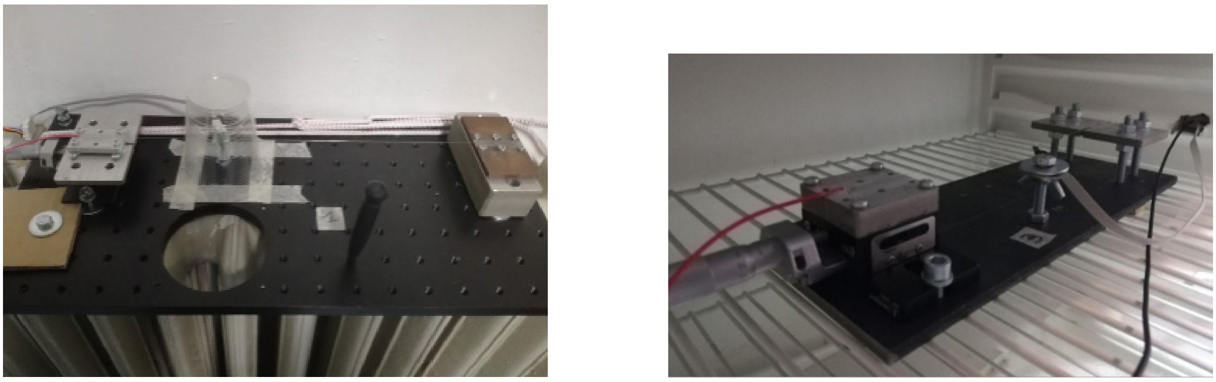

(a) "Radiator" measuring station (b) "Fridge" measuring station

Figure 2: Radiator and Fridge measuring stations

The FBGs sensors are the focus of this work. Three different optical lines are sued in this testing setup, each one in on of the three measuring stations. FBGs used in this setup have nominal wavelength of 1545 nm or 1550 nm. Thanks to the setup nature, with three different and independent supports each one connected to a different interrogator channel, it is acceptable to have one sensor with a different nominal wavelength.

The mechanical support frames are metallic plates where the FBGs sensors are glued on top. Furthermore, all the fibers are pre-tensioned using micro-handlers; in fact, fiber (and thus FBGs) pre-tensioning value is of fundamental importance in order to correlate the variation in Bragg wavelength $\Delta\lambda_B$ with the actual fiber strain $\Delta\varepsilon$. The mechanical bonding between fibers and supports is made using Araldite 2011. It is an epoxy-based adhesive that undergoes polymerization at ambient temperature. Thus, the glue has very good tenacity and good resistance, which are good characteristics in this test setup, where loads are applied for long periods of time. Low shrinkage and high shear stiffness also minimize the error introduced on the sensor measures.

The FBG interrogator is a device that sends a laser beam to the FBG sensor and detect the reflected wavelength. Furthermore, the interrogator has several different channels in order to separate the various FBG measurements. In this setup, SmartScan SBI laser interrogator was used, developed by SmartSoft Fibres. The results shown in this work are managed by SmartScan software, SmartSoft. The data acquisition loop will be carried out every 10 minutes; each measurements will span 10 seconds with a sampling frequency of 25 kHz. All the data will then be averaged to obtain the average wavelength in that measuring window. Accuracy and resolution of the measure are function of the laser bandwidth and the post-processing methods selected. Normal values ranges are about 1 pm in wavelength, corresponding to about 1 microstrain or a variation of 0.1 ^oC.

The electrical power unit provides energy for interrogator operations; it has two output channels. Maximum current output is 2 A, while max voltage is limited at 60 V for the first channel and 30 V for the second channel.

Each FBG sensor is combined with a SHT85 sensor which simultaneously acquires local ambient temperature and relative humidity values (thus measuring the environmental conditions where the FBG operates). The sensor has an temperature range between - 40 and + 105 °C and measures relative humidity values from 0% to 100%. The nominal accuracy of the SHT85 sensor is equal to ±1.5% for relative humidity and ±0.1 ^oC for temperature measurement. Sensors will acquire relative humidity and temperature values for 10 seconds in each measurement loop.

Finally, the ARDUINO UNO microcontroller is the electronic board that shall receive and communicate data acquired by SHT85 sensors. It transfer information regarding sensors logged data to the PC using a USB datalink. Said data will then be saved, using a MATLAB script that pairs them with the data obtained by the SmartScan SBI interrogator on the measured reflected wavelength of each FBG.

In Fig. 3, a preliminary measurement set, carried out for a single day, for a single station, is presented. In Fig. 3a and Fig. 3b, the environmental data of interest (i.e. temperature and relative humidity, respectively) are plotted; these data are obtained, as previously stated, using the SHP85 sensor. Finally, in Fig. 3c, the reflected wavelength data, obtained using the SmartScan interrogator, are plotted. It has to be noted that both environmental data and optical data are sampled at the same time intervals in order to allow easy post processing (i.e. no need to interpolate for missing time values).

4. Conclusions

In this work, a test setup to analyze the effect of environmental conditions variations on FBG optical sensors has been presented. Three different measuring stations are present in order to carry out parallel measurements in different conditions of temperature and relative

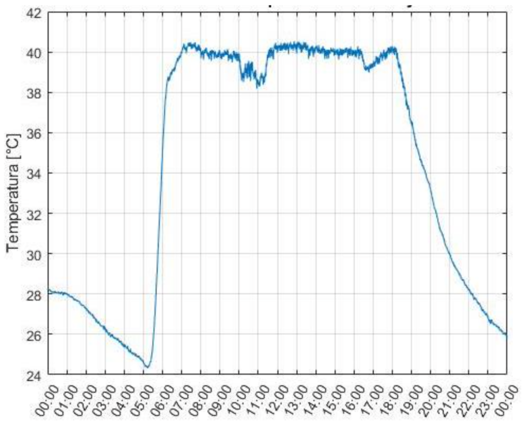

(a) Temperature log

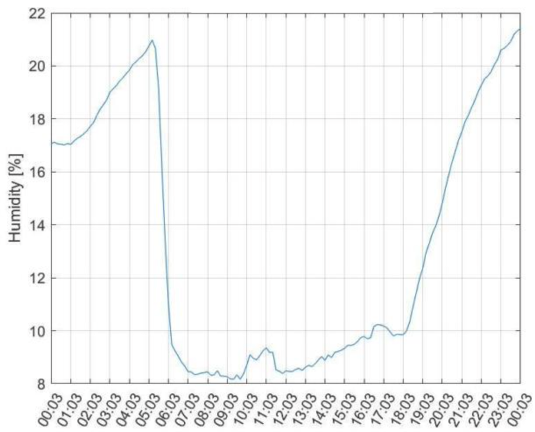

(b) Relative humidity log

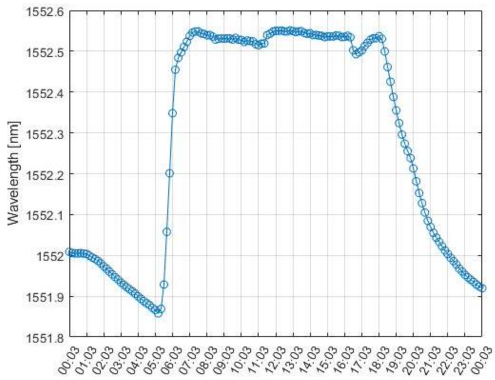

(c) Wavelength log

Figure 3: Preliminary environmental and wavelength measurement for "Radiator" station (10/01/2020)

humidity. Preliminary testing on a single station (Fig. 3), seems to suggest a correlation between temperature and wavelength, while the relation between relative humidity and reflected wavelength is not immediately apparent.

Since the scope of this work, as said before, is to characterize time-dipendent, non-linear effect arising from the mechanical bonding using epoxy glue, the data logging will have to be carried out for long periods of time and then post-processed to obtain any possible time evolution of the fiber-glue-support system behavior.

References

[1] Anderson R J and Aylward S R 1993 Lab testing of neural networks for improved aircraft onboard-diagnostics on flight-ready hardware *Annual Reliability and Maintainability Symposium 1993 Proceedings* (IEEE) pp 404–410
[2] Quattrocchi G, Berri P C, Dalla Vedova M D and Maggiore P 2020 *Actuators* **9** 50
[3] De Martin A, Jacazio G and Vachtsevanos G 2017 *Int. J. Progn. Heal. Manag* **8**
[4] Dalla Vedova M D, Germanà A, Berri P C and Maggiore P 2019 *Aerospace* **6** 94
[5] Hasan A and Johansen T A 2018 Model-based actuator fault diagnosis in multirotor uavs *2018 International Conference on Unmanned Aircraft Systems (ICUAS)* (IEEE) pp 1017–1024
[6] Berri P C, Dalla Vedova M D and Maggiore P 2016 *International Journal of Mechanics and Control* **17** 19–25
[7] Berri P C, Dalla Vedova M D and Mainini L 2018 Diagnostics of actuation system faults from dynamic

data *Proceedings of the 6th European Conference on Computational Mechanics (ECCM 6), European Community on Computational Methods in Applied Sciences (ECCOMAS), Glasgow, UK* pp 11–15

[8] Berri P, Dalla Vedova M and Maggiore P 2017 On-board electromechanical servomechanisms affected by progressive faults: proposal of a smart ga model-based prognostic approach *Proc. of the 27th European Safety and Reliability Conference* (Portoroz Slovenia) pp 839–845

[9] Byington C S, Watson M, Edwards D and Stoelting P 2004 A model-based approach to prognostics and health management for flight control actuators *2004 IEEE aerospace conference proceedings (IEEE Cat. No. 04TH8720)* vol 6 (IEEE) pp 3551–3562

[10] Vachtsevanos G J and Vachtsevanos G J 2006 *Intelligent fault diagnosis and prognosis for engineering systems* vol 456 (Wiley Hoboken)

[11] Mihailov S J 2012 *Sensors* **12** 1898–1918

[12] Xin G, Zhengying L, Fan W, Yiming W, Changjia W, Siyue Z and Haihu Y 2017 *Optics Express* **25** 28112–28122

[13] Tanaka N, Okabe Y and Takeda N 2003 *Smart materials and structures* **12** 940

[14] Brusa E, Vedova M D, Giorio L and Maggiore P 2019 *Mechanics of Advanced Materials and Structures* 1–7

[15] Dalla Vedova M, Berri P, Maggiore P and Quattrocchi G 2020 Design and development of innovative fbg-based fiber optic sensors for aerospace applications *Journal of Physics: Conference Series* vol 1589 (IOP Publishing) p 012012

[16] Quattrocchi G, Berri P, Dalla M V and Maggiore P 2021 Optical fibers applied to aerospace systems prognostics: design and development of new fbg-based vibration sensors *IOP Conference Series: Materials Science and Engineering* vol 1024 (IOP Publishing) p 012095

[17] Liu L, Zhang H, Zhao Q, Liu Y and Li F 2007 *Optical fiber technology* **13** 78–80

[18] Kisala P and Cieszczyk S 2015 *Applied Optics* **54** 2677–2687

[19] Zhou Z and Ou J 2005 Techniques of temperature compensation for fbg strain sensors used in long-term structural monitoring *Fundamental Problems of Optoelectronics and Microelectronics II* vol 5851 (International Society for Optics and Photonics) pp 167–172

[20] Wang W, Yu Y, Geng Y and Li X 2015 Measurements of thermo-optic coefficient of standard single mode fiber in large temperature range *2015 International Conference on Optical Instruments and Technology: Optical Sensors and Applications* vol 9620 (International Society for Optics and Photonics) p 96200Y

[21] Krohn D A, MacDougall T and Mendez A 2014 *Fiber optic sensors: fundamentals and applications* (Spie Press Bellingham, WA)

[22] Kreuzer M 2006 *HBM, Darmstadt, S2338-1.0 e* 12